PHILOSOPHICAL TRANSACTIONS OF THE ROYAL SOCIETY A MATHEMATICAL, PHYSICAL & ENGINEERING SCIENCES

Experimental Results on Atmospheric Neutrinos

E. W. Beier and E. D. Frank

Phil. Trans. R. Soc. Lond. A 1994 **346**, 63-73
doi: 10.1098/rsta.1994.0007

Experimental results on atmospheric neutrinos

By E. W. Beier and E. D. Frank

Department of Physics, University of Pennsylvania, Philadelphia, PA 19104-6396, U.S.A.

Atmospheric neutrinos arise from the decay of mesons produced by the interactions of high energy cosmic rays with nuclei in the Earth's atmosphere. Studies of the interactions of these neutrinos are sensitive to the fundamental properties of neutrinos such as neutrino mass and neutrino flavour mixing. Because the energies of these neutrinos range from less than 1 GeV to more than 10 TeV, and because the distances from the production site to the detector range from 10 to 10000 km, the range of neutrino mass differences sampled is large and extends to lower values than is presently accessible to accelerator experiments. This paper summarizes the status of experimental results on atmospheric neutrinos and the possible interpretations of these results.

1. Introduction

Atmospheric neutrinos arise from the decay of mesons and leptons that are produced in primary and secondary interactions of high energy cosmic ray particles with nuclei in the atmosphere. For a neutrino detector located at the surface of the Earth, the distance from the production point of the neutrino to the detector can range from 10 km for a neutrino produced at zenith to 10^4 km for one produced near nadir. The energies of the neutrinos range from a few MeV to many TeV. If the flux of produced neutrinos is well understood, the ranges of energies and path lengths permit, through the process of neutrino flavour oscillations, studies of neutrino mass and neutrino flavour mixing in régimes not accessible to date using terrestrial neutrino sources. This is the principle emphasis in the interpretation section of the present review.

Calculation of the flux of atmospheric neutrinos is the subject of another contribution to this volume (Gaisser). For the purpose of the immediate discussion, it suffices to say that the neutrinos arise primarily from the decay of produced pions, and at energies above a few GeV, produced kaons, through the modes $(\pi^+, K^+) \rightarrow \mu^+\nu_\mu$ followed by the decay of the muon $\mu^+ \rightarrow e^+ + \nu_e + \bar{\nu}_\mu$, and similarly for (π^-, K^-). In energy régimes of interest for the contained event studies discussed below, the neutrino flux ratio averaged over all angles, $R_\phi = \phi(\nu_\mu + \bar{\nu}_\mu)/\phi(\nu_e + \bar{\nu}_e)$, is predicted to be close to $R_\phi \approx 2$ with an uncertainty in the calculation of 5%, while the uncertainty in the absolute flux is 20–30%. This robust prediction of the flux flavour ratio makes the atmospheric neutrinos amenable to the study of flavour oscillation.

Turning now to the experiments, two types of event sample have been analysed. The first type, in which all of the products of each interaction are completely contained within a massive, large volume detector, is referred to as a 'contained event' sample. Atmospheric neutrinos, incident almost isotropically, produce approximately 100 contained events per kilotonne-year (kt-yr), but depending on geomagnetic latitude and the acceptance of the detector. Detectors constructed to

Phil. Trans. R. Soc. Lond. A (1994) **346**, 63–73
Printed in Great Britain

date are either water Čerenkov detectors in which the neutrino target is a large volume of water viewed by a surface array of photomultiplier tubes, or iron plate calorimeters in which charged particles produced by the neutrino interaction ionize gas between the iron plates, allowing images of the paths of the reaction products to be reconstructed electronically. The detectors are located deep underground to reduce the rate of events from downward going cosmic ray muons. Existing detectors do not measure the sign of the charged lepton $l^{\pm}$ and thus do not distinguish ν_l from $\bar{\nu}_l$. In what follows, ν will refer to either ν, $\bar{\nu}$, or both.

The mean energy of neutrinos producing contained events is approximately 1 GeV. Within the contained event sample, events labelled as having a single observed particle, either an electromagnetic shower or a non-showering particle, are predominantly ν_μ or ν_e quasi-elastic scattering. Events consistent with this simple topology are often chosen for study because the quasi-elastic cross section is understood well. In fact, at neutrino energies $E_\nu \leqslant 5$ GeV, characteristic of the contained events, the exclusive cross sections and the total cross section are measured well enough (Nakahata 1986) that the total number of events observed relative to those with a single track or shower also constrains the interpretation of the data (Frank 1992).

The second type of event sample utilizes the material beneath a detector as the neutrino target. High energy atmospheric neutrinos of muonic flavour produce secondary muons and hadrons in the target material. The hadrons are absorbed in the target material, but the high energy muons can reach the detector. The detected muons usually traverse the detector, but sometimes a muon will stop in the detector. The former will be called 'upward through muons', and the latter will be called, 'upward stopped muons'. Together the two will be called 'upward muons'. Only upward going muons are selected because the number of downward going muons produced by neutrinos is small compared to the number of cosmic ray muons and cannot be distinguished from them. The produced muons propagate in a direction close to that of the incident neutrino.

The mean energy of the neutrinos that produce upward through muons is about 100 GeV, while the mean energy of neutrinos that produce upward stopped muons is about 10 GeV. The ratio of stopped to through upward muons in a detector has reduced sensitivity to the absolute calculated flux of neutrinos (Becker-Szendy 1992*b*). The ratio is sensitive to differences in the shape of the energy spectrum between different calculations of the neutrino flux, for example, through different assumptions about the relative production rates of K and π mesons. A third example of a quantity which is insensitive to the absolute neutrino flux is the zenith angle distribution of the observed muons, although no experiment yet has sufficient statistics to exploit this distribution. It would be useful to have quantitative estimates of the uncertainty in the expected zenith angle distribution before future large acceptance detectors begin taking data.

The following sections review the existing contained event and upward muon atmospheric neutrino data. The contained event data are often interpreted by authors using the flux calculations of Gaisser, Stanev, and collaborators (Gaisser 1988; Barr 1989; Honda, *et al.* 1990; Lee & Koh 1990; Bugaev & Naumov 1987, 1989). Flux calculations of atmospheric neutrinos used to date for the study of much higher energy régimes relevant to upward muons include those of Butkevich (1989) and Volkova (1980). A synthesis of the results of the experiments, comments, and a discussion of future work conclude this paper.

PHILOSOPHICAL TRANSACTIONS OF THE ROYAL SOCIETY A MATHEMATICAL, PHYSICAL & ENGINEERING SCIENCES

2. Results on contained events

Results have been reported on contained event samples for two large water Čerenkov detectors and two iron plate calorimeters. The water Čerenkov detectors have by far the largest exposures, and will be presented first.

(*a*) *The Kamiokande and IMB water Čerenkov data*

The Kamiokande collaboration (Hirata 1988, 1992; Kajita 1993) has reported data from a 6.18 kt-yr exposure of the Kamiokande I, II, and III configurations of their water Čerenkov detector. Containment is defined by a requirement limiting the maximum pulse height in a single photomultiplier, and in the Kamiokande II and III configurations, by also limiting the activity in a 4π steradians, hermetic veto counter. Each charged particle above Čerenkov threshold produces Čerenkov light in a ring pattern. The light produced by all charged particles above Čerenkov threshold is detected by the photomultiplier tubes on the surface of the detector.

The data are first separated into subsets of events consistent with single ring and multi-ring hypotheses by scanning. The single ring events are then separated into e-like (e^+, e^-, and γ) or μ-like (μ^+, μ^-, and heavier particles) using algorithms that distinguish the diffuse nature of the Čerenkov ring in an electromagnetic shower from the sharper ring made by a non-scattering particle such as a muon. The single-ring and multi-ring separation error and the particle type misidentification are both estimated from Monte Carlo (MC) simulations to be as small as 2% (Kajita 1993). Once the particle type is identified, the charge collected in the photomultipliers, suitably corrected for attenuation of the Čerenkov light and detector geometry, is used to determine the momentum of the particle. Calibration of the momentum scale is performed using Čerenkov light from through going cosmic ray muons, stopped cosmic ray muons, and electrons produced in the decay of stopped muons.

Monte Carlo simulation of the events predicts that the single ring e-like (μ-like) events are about 95% charged current ν_e (ν_μ) induced, the remainder being neutral current events. Quasi-elastic scattering accounts for 75% of the single ring samples. Thus the single ring data samples are predicted to be well understood ν_μ and ν_e interactions. By comparing the ratio of $(\mu/e)_{data}$ to $(\mu/e)_{MC}$ for the single ring samples, sensitivity to the calculation of the absolute flux is minimized when making a flavour assay of the neutrino flux. Here (μ/e) is the ratio of the number of μ-like to e-like events.

A confirmatory measure of the flavour content of a sample of events is provided by the observation of the electron from the decay of produced, contained muons. The decay detection efficiency is 89% in Kamiokande II, III, and 76% in Kamiokande I. This efficiency is well understood from measurements of stopped cosmic ray muons. The Kamiokande collaboration reports a muon decay analysis for the single ring subset of the data (Hirata 1992; Kajita 1993). The muon decay flavour assay is independent of the particle identification technique and yields results consistent with that technique.

From a total of 578 fully contained events, 410 are determined to be single ring events, of which 191 are μ-like events in the momentum interval $0.20 < p_\mu < 1.50$ GeV c^{-1} and 198 are e-like events in the momentum interval $0.10 < p_e < 1.33$ GeV c^{-1}. A summary of these data and a comparison to the expectation using the largest neutrino flux (Barr 1989) and the smallest neutrino flux (Lee 1990) is given in table 1. The expectation is calculated from the stated neutrino flux, a Fermi

PHILOSOPHICAL TRANSACTIONS OF THE ROYAL SOCIETY A MATHEMATICAL, PHYSICAL & ENGINEERING SCIENCES

PHILOSOPHICAL TRANSACTIONS OF THE ROYAL SOCIETY A MATHEMATICAL, PHYSICAL & ENGINEERING SCIENCES

Table 1. *A summary of the contained event data*
(NA, not applicable.)

	exposure		momentum	data		(Barr 1989) flux		(Lee 1990) flux		$\frac{(\mu/e)_{data}}{(\mu/e)_{MC}}$
experiment	kt-yr	event type	GeV c^{-1}	total	$\mu \to e$	total	$\mu \to e$	total	$\mu \to e$	
Kamiokande	6.18	μ-like	0.2–1.20	191	126	325	231	256	—	$0.60 \pm 0.06 \pm 0.05$
		e-like	0.1–1.33	198	16	203	22	157	—	—
		multi-ring	NA	168	64	208	86	—	—	—
IMB	7.70	μ-like	0.3–1.5	182	117	345	—	268	180	$0.55 \pm 0.05 \pm$?
		e-like	0.1–1.5	325	51	340	—	257	43	—
		multi-ring	NA	325	137	319	—	240	116	—
NUSEX	0.74	μ-like	> 0.2	32	—	36.8	—	—	—	0.99 ± 0.29
		e-like	> 0.2	18	—	20.5	—	—	—	—
Frejus	1.56	μ-like	> 0.2	108	—	125.8	—	—	—	$1.06 \pm 0.18 \pm 0.15$
		e-like	> 0.2	57	—	70.6	—	—	—	—
Frejus (contained)		μ-like	> 0.2	66	—	90.0	—	—	—	$0.87 \pm 0.16 \pm 0.12$
		e-like	> 0.2	56	—	66.8	—	—	—	—

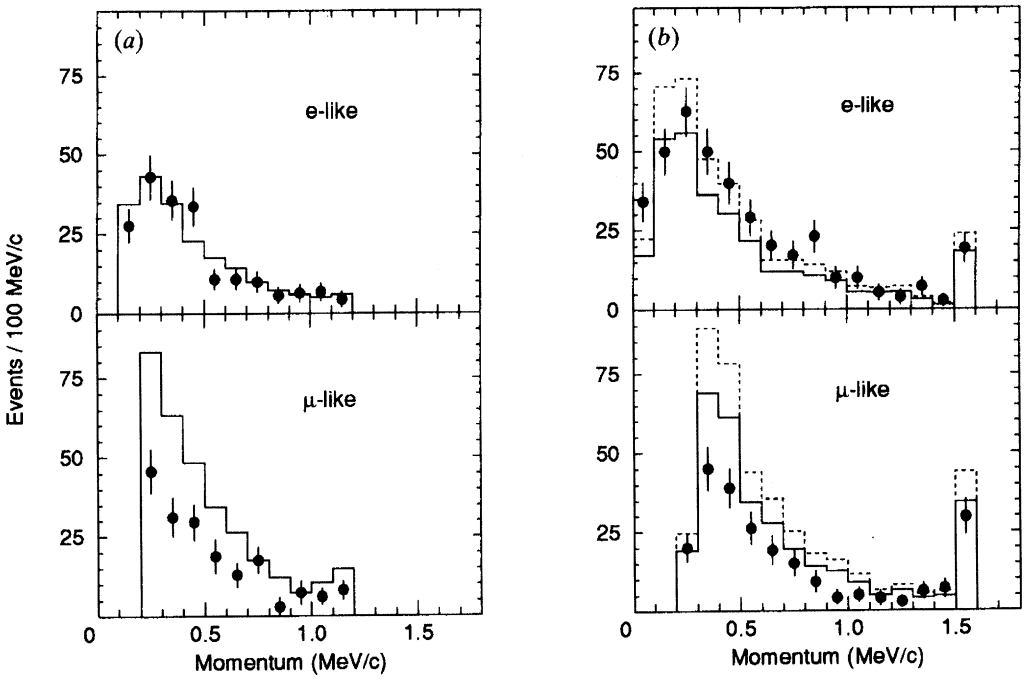

Figure 1. Momentum spectra for contained, single-ring events in the imaging water Čerenkov detectors (*a*) Kamiokande (6.18 kt-yr) and (*b*) IMB (7.7 kt-yr), adapted from Kajita (1993) and Becker-Szendy (1992*a*). The solid histograms are the fluxes preferred by the original authors; Barr (1989) for Kamiokande and Lee (1990) for IMB. The dashed line for IMB is the estimate for Barr (1989) that is described in the text.

gas model of the interaction of neutrinos with ^{16}O, and the simulated response of the Kamiokande detector. The momentum distributions of the Kamiokande e-like and μ-like events are shown in the left-hand boxes of figure 1. The solid histogram shows the expectation using the Barr *et al.* (1989) neutrino flux. The events in the highest momentum bin are the sum of all events with momentum greater than 1.10 GeV c^{-1}.

The IMB collaboration (originally Irvine, Michigan, Brookhaven) has published the results of a study of contained events from a 7.7 kt-yr exposure of a second water Čerenkov detector, the IMB-3 detector (Becker-Szendy 1992*a*). Two independent analyses using software algorithms and scanning of event displays were used to determine a sample of contained events. Assuming independence of the two analyses, the efficiency for recovering contained events was 93%. From a sample of 935 contained events, 610 were classified as single ring events and the remaining 325 were classified as multiple ring events. The single ring events were classified as showering (e-like) or non-showering (μ-like) using the combined results of three software algorithms. Studies using cosmic rays and Monte Carlo simulations indicate that $(92 \pm 5)\%$ of single ring events were identified correctly where the uncertainty is systematic (Casper 1991). There is negligible net bias toward either classification. The redundant flavour assay using electrons from the decay of produced muons is consistent with the particle type classification. From the Monte Carlo simulation, the events identified as μ-like are 92% charged current ν_μ induced and the events identified as e-like are 87% charged current ν_e induced.

The analysis finds 325 e-like events in the momentum interval $0.10 < p_e <$

1.50 GeV c^{-1} and 182 μ-like events in the momentum interval $0.30 < p_\mu < 1.50$ GeV c^{-1}. The momentum distribution of these events is displayed in the right-hand boxes of figure 1. The highest momentum bin represents the sum of all events with momentum greater than 1.50 GeV c^{-1}. The expected distributions, analogous to those in the Kamioka data, are shown for the Lee & Koh flux (solid histogram) and the Barr flux (dashed line histogram). The Barr spectra for the IMB data in figure 1 was obtained by scaling the Lee spectra reported in (Becker-Szendy 1992*a*) by 1.31 for e-like and 1.28 for μ-like spectra according to table 1 of (Casper 1991).

(*b*) *The NUSEX and Fréjus iron calorimeter data*

Two collaborations have reported data from underground iron calorimeters. The NUSEX collaboration has reported data from a 0.74 kt-yr exposure of a detector in the Mt Blanc tunnel (Aglietta 1989), and the Fréjus collaboration has reported data from a 1.56 kt-yr exposure of a detector in the Fréjus tunnel between France and Italy (Berger 1989, 1990).

In these experiments, contained events are defined by the absence of activity near the boundary of the calorimeter volume. The Fréjus collaboration has obtained both a sample of contained events, and an additional sample of events in which the lepton is identified, but exits the detector. Identification of μ-like and e-like events is accomplished by distinguishing the electromagnetic cascade of electrons and photons from the penetrating track of a muon. Test modules of both detectors have been calibrated in particle beams at accelerators.

A summary of the data from the contained event samples is displayed in table 1, including data from both the water Čerenkov detector and the iron calorimeter experiments. The Monte Carlo predictions in table 1 are with respect to the Barr (1989) flux except for the NUSEX prediction which is with respect to the same flux before the inclusion of the effect of muon polarization (Gaisser 1988). Comparison of these two calculations indicates that including the polarization increases the expected number of e-like events relative to μ-like events by about 10–15% (Barr 1989). The Barr flux expectation for the 7.7 kt-yr IMB exposure was obtained by scaling the expectation for the 3.4 kt-yr exposure (Casper 1991). The IMB data in table 1 cannot be compared directly to the Kamiokande data because the momentum intervals and acceptances are different. If the Kamiokande and IMB data are taken for the same lepton momentum interval $0.30 < p < 1.1$ GeV c^{-1}, then the central values of the ratio of ratios, $\mathscr{R} = (\mu/e)_{data}/(\mu/e)_{MC}$, become 0.57 and 0.47, respectively. Since $\mathscr{R} \neq 1.0$, there is a discrepancy between data and expectation. This discrepancy is the atmospheric neutrino problem.

3. Results on upward muons

Analyses of data samples of upward through muons have been presented by the Kamiokande collaboration (Oyama 1989; Mori 1991) the IMB collaboration (Becker-Szendy 1992*a*), and by the Baksan underground scintillation telescope collaboration (Boliev 1991), located in the Baksan Neutrino Observatory in the Caucasus mountains in Russia. All three of the experiments measured the rate of upward through muons as a function of zenith angle. The IMB collaboration was also able to measure the rate of upward stopped muons in their detector. The muon detection threshold and the observed number of events for each data-set are given in table 2.

PHILOSOPHICAL TRANSACTIONS OF THE ROYAL SOCIETY A MATHEMATICAL, PHYSICAL & ENGINEERING SCIENCES

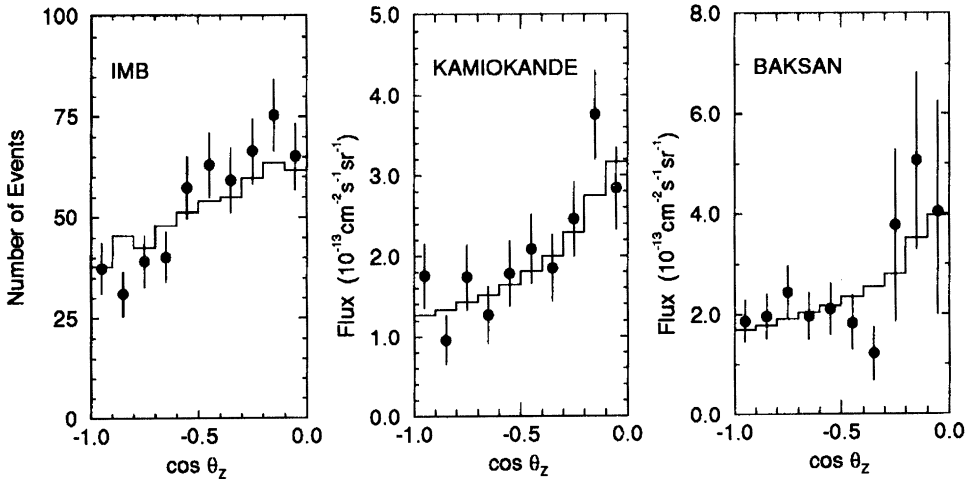

Figure 2. Zenith angle distributions for three upward-going muon experiments, adapted from Svoboda (1993), Mori (1991) and Boliev (1991). A muon travelling upwards in the detector is plotted at -1.0 in these figures.

Table 2. *A summary of date on upward going muons*

	muon threshold	
experiment	GeV	number of events
Kamiokande	1.7	252
IMB 1, 2 (3)	1.8 (1.0)	532 through
	1.0	85 stopped
Baksan	1.0	421

The zenith angle distributions for the three experiments are displayed in figure 2. The large error bars near the horizontal for the Baksan distribution is a result of limited detection efficiency. The Baksan collaboration uses a muon energy threshold of 1 GeV, while the Kamiokande collaboration requires a threshold of 1.7 GeV. The IMB data include configurations of the detector, IMB 1, 2 and 3, which have two different thresholds. For the IMB data, the number of events as a function of zenith angle is plotted. The differential flux of upward going muons as a function of zenith angle is plotted for the Kamiokande and Baksan experiments.

The histograms for each of the distributions in figure 2 represent the expected number of events or muon flux calculated by the original authors using the neutrino flux calculation of Volkova. The different collaborations have used different combinations of muon energy loss and neutrino cross sections in arriving at the calculated distributions.

4. Interpretation and conclusions

The data discussed above can be used to study neutrino flavour transformation in a neutrino mass regime which has not been explored by reactors or accelerators to date. Many of the authors of the papers discussed above have analysed their data in terms of two flavour mixing, studying the neutrino properties $\Delta m^2 = |m_2^2 - m_1^2|$ and $\sin^2 2\theta$, where m_1 and m_2 are masses of two neutrino mass eigenstates, and θ is the

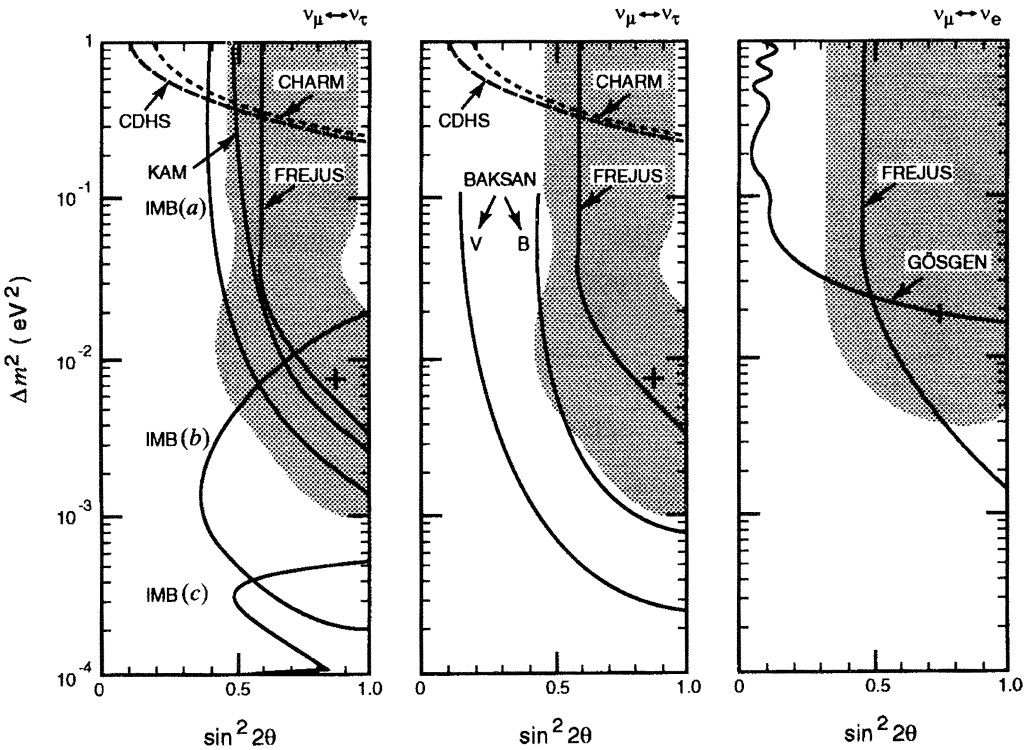

Figure 3. Neutrino flavour mixing contours at 90% confidence level for several experiments, adapted from Hirata (1992). The grey areas are allowed by the Kamiokande contained data while the regions to the right of the solid curves are excluded by the corresponding experiment. The notation is defined in the text.

vacuum mixing angle between the eigenstates. The data have been used to study flavour transformation of two types, $\nu_e \leftrightarrow \nu_\mu$ and $\nu_\mu \leftrightarrow \nu_\tau$. This is accomplished through the use of the appropriate flavour transition probability, for example

$$P(\nu_\mu \leftrightarrow \nu_\tau) = \sin^2 2\theta \sin^2 (\Delta m^2 L/4E_\nu), \tag{1}$$

where L is the distance between the source of neutrinos and the target and E_ν is the neutrino energy.

Allowed and excluded contours in $\Delta m^2, \sin^2 2\theta$ space produced by the various collaborations are displayed in three plots in figure 3 for $\nu_\mu \leftrightarrow \nu_\tau$ and $\nu_e \leftrightarrow \nu_\mu$ flavour transformations. The shaded area in all the plots is the 90% confidence level allowed region defined by the first 4.92 kt-yr of the Kamiokande contained event data (Hirata 1992). The cross indicates the location of the minimum χ^2 for a simultaneous fit to the momentum and zenith angle distributions. The minimum χ^2 for $\nu_\mu \leftrightarrow \nu_\tau$ occurs at $\Delta m^2 = 0.8 \times 10^{-2}$ eV^2, $\sin^2 2\theta = 0.87$, and similar values for $\nu_e \leftrightarrow \nu_\mu$ where matter effects have been included. The IMB collaboration has not published a neutrino oscillation analysis of the IMB 3 contained event data and Kamiokande has not published a new analysis for the full 6.18 kt-yr sample.

The area to the right of each solid line is excluded at 90% confidence level by the indicated experiment. In the left most plot the curve labelled IMB(a) is deduced from the upward through muons (Becker-Szendy 1992b), that labelled IMB(b) is from the ratio of upward stopped muons to upward through muons (Becker-Szendy

PHILOSOPHICAL TRANSACTIONS OF THE ROYAL SOCIETY A MATHEMATICAL, PHYSICAL & ENGINEERING SCIENCES

1992*b*), and that labelled IMB (*c*) is obtained from a sample of IMB 1 contained single ring events with an associated electron from a muon decay (Bionta 1988). Also in the left most plot, the curve labelled KAM is deduced from the Kamiokande I and II upward through muons (Oyama 1989; Mori 1991). The $\nu_\mu \leftrightarrow \nu_\tau$ plot is displayed twice so that exclusion contours of different experiments can be distinguished. Shown separately in the centre plot are two exclusion curves deduced from the Baksan upward through muon data in the restricted angular range $-1.0 < \cos\theta_Z < -0.6$, although they selected a different restricted angular range $-0.8 < \cos\theta_Z < -0.5$ for their $\nu_e \leftrightarrow \nu_\mu$ analysis (Boliev 1991). The curve labelled 'B' is obtained using the Butkevich *et al.* neutrino flux (Butkevich 1989), and that labelled 'V' is obtained from the smaller Volkova flux (Volkova 1980), thereby showing the sensitivity of the exclusion contour to the neutrino flux uncertainty. The Fréjus exclusion curve is shown in all three plots (Berger 1990). Also shown on the left two plots are the exclusion contours for ν_μ disappearance deduced from the CDHS (Dydak 1984) and CHARM (Bergsma 1984) accelerator experiments and, in the right most plot, the Gösgen (Zacek 1986) $\bar{\nu}_e$ reactor experiment.

With respect to the upward through muons, the Baksan collaboration appears to have chosen the zenith angle region to maximize the excluded region since the choice is different for $\nu_\mu \leftrightarrow \nu_\tau$ and $\nu_\mu \leftrightarrow \nu_e$ (Boliev 1991). Frati *et al.* (1993) and Perkins (1993) have addressed the uncertainties in the predicted event rates for upward going muons. Frati *et al.* argue that when more current data for the input to the flux calculations and cross sections for the upward muon data are used, less of the region allowed by Kamiokande in figure 3 is excluded. These uncertainties are addressed in more detail in Gaisser's contribution to these proceedings. Perkins has emphasized the use of experimental data in the event rate estimates, and his choices lead to significantly lower expected rates than those of Frati *et al.* The exclusion region defined by the IMB ratio of stopped to through going upward muons is less sensitive to these uncertainties, but is not completely independent of them. The uncertainties to date are such that not all of the Kamiokande allowed region is in conflict with the data from upward going muon experiments when the two types of data are analysed separately.

The argument that the iron calorimeter contained event data contradicts the water Čerenkov data is not statistically compelling if one simply looks at the ratio $(\mu/e)_{data}/(\mu/e)_{MC}$ in table 1, but the Fréjus data permit 90% confidence level exclusion contours (shown in figure 3) and 95% confidence level contours to be drawn (Berger 1990). Given so many experiments, it would be useful to require stricter statistical standards, such as 99.5% confidence levels for plots like figure 3. Successful execution of such a program will require that experiments not be systematics limited. The Fréjus data have also raised a concern that the analyses of the collaborations operating the water Čerenkov detectors could be missing some systematic effects in common.

The Kamiokande contained event data are consistent with the hypothesis of neutrino oscillations. For $\nu_\mu \leftrightarrow \nu_\tau$, the absolute number of e-like and μ-like events, the shapes of the e-like and μ-like momentum spectra, and the zenith angle distributions agree with the Barr flux expectation when oscillations are included (Hirata 1992). The IMB contained event data do not fit these criteria as well, as can be seen from the shapes of the e-like data and e-like expected momentum distribution in figure 1. This inconsistency between two data-sets which both show similar discrepancies with respect to expectations is a concern which should be addressed. Systematic

PHILOSOPHICAL TRANSACTIONS OF THE ROYAL SOCIETY A MATHEMATICAL, PHYSICAL & ENGINEERING SCIENCES

experimental differences could be uncovered by the planned joint Kamiokande and IMB program to calibrate the response of their detectors to charged particle and neutrino beams at KEK.

One can consider possibilities other than neutrino oscillations, as the explanation for the unexpected μ/e ratio in the contained event samples. Nuclear effects could change the absolute cross sections, but it is difficult to change the flavour ratio since the data are at a high enough energy that the kinematic differences between μ and e are not important (Engel 1993; A. K. Mann 1993). It has also been suggested that proton decay $p \rightarrow e^{+}\nu\nu$ could produce an excess of electrons (W. A. Mann *et al.* 1992). If some new, unspecified, ν_e flux is to account for the data, it must have an energy spectrum very similar to that of the known atmospheric ν_e spectrum.

Future experimental prospects for understanding atmospheric neutrinos include a 5 kt-yr exposure of the new Soudan 2 iron calorimeter detector, now operational in northern Minnesota. That detector will have a sample of contained events with completely different systematic errors from those of the water Čerenkov detectors. On the same timescale, the SuperKamiokande detector with a fiducial volume twenty two times that of Kamiokande should have a two year or 44 kt-yr exposure, producing sufficient statistics to perform detailed studies of systematic effects.

It is incumbent upon those active in the field to resolve the existing uncertainties associated with the present measurements. Perhaps new measures less susceptible to calculational uncertainties can be found, such as the rate of contained μ-like events relative to upward stopped muons. Precise data to constrain the uncertainties in neutrino flux calculations are also needed. Perhaps the legacy of the study of atmospheric neutrinos will be a series of long baseline accelerator experiments where one can calibrate the detectors and perform control experiments. This may be the only way to determine whether the effects of fundamental properties of neutrinos are being observed in the existing atmospheric neutrino data.

This work was supported by the United States Department of Energy. We thank our former collaborators in the Kamiokande II experiment and our IMB colleagues for useful discussions.

References

Aglietta, M., *et al.* 1989 Experimental study of atmospheric neutrino flux in the NUSEX experiment. *Europhys. Lett.* **8**, 611–614.

Barr, G., Gaisser, T. K. & Stanev, T. 1989 Flux of atmospheric neutrinos. *Phys. Rev.* D **39**, 3532–3534.

Becker-Szendy, R., *et al.* 1992*a* Electron- and muon-neutrino content of the atmospheric flux. *Phys. Rev.* D **46**, 3720–3724.

Becker-Szendy, R., *et al.* 1992*b* Search for muon neutrino oscillations with the Irvine–Michigan–Brookhaven detector. *Phys. Rev. Lett.* **69**, 1010–1013.

Berger, Ch., *et al.* 1989 Study of atmospheric neutrino interactions with the Fréjus detector. *Phys. Lett.* B **227**, 489–494.

Berger, Ch., *et al.* 1990 A study of atmospheric neutrino oscillations in the Fréjus experiment. *Phys. Lett.* B **245**, 305–310.

Bergsma, F., *et al.* 1984 A search for oscillations of muon neutrinos with $L/E \simeq 0.7$ km/GeV. *Phys. Lett.* B **142**, 103–110.

Bionta, R. M., *et al.* 1988 Contained neutrino interactions in an underground water detector. *Phys. Rev.* D **38**, 768–775.

Boliev, M. M., Butkevich, A. V., Chudakov, A. E., Mikheyev, S. P., Skarzhinskaya, N. V. & Zakidyshev, V. N. 1991 Baksan high energy neutrino experiment. In *Proc. of the Third*

International Workshop on Neutrino Telescopes (ed. M. Baldo Ceolin), pp. 235–245. Padova: CLEUP.

Bugaev, E. V. & Naumov, V. A. 1989 On the interpretation of the Kamiokande neutrino experiment. *Phys. Lett.* B **232**, 391–397.

Bugaev, E. V. & Naumov, V. A. 1987 Cosmic ray muons and neutrinos at low and intermediate energy. *Yad. Fiz* **45**, 1380–1391. (Trans. *Sov. J. Nucl. Phys.* **45**, 857–864.)

Butkevich, A. V., Dedenko, L. G. & Zheleznykh, I. M. 1989 Spectra of hadrons, muons, and neutrinos in the atmosphere as the solution of a direct problem. *Yad. Fiz.* **50**, 142–156. (Trans. *Sov. J. Nucl. Phys.* **50**, 90–99.)

Casper, D., *et al.* 1991 Measurement of atmospheric neutrino composition with the IMB-3 detector. *Phys. Rev. Lett.* **66**, 2561–2564.

Dydak, F., *et al.* 1984 A search for ν_μ oscillations in the Δm^2 range 0.3–90 eV^2. *Phys. Lett.* B **134**, 281–286.

Engel, J., Kolbe, E., Langacke, K. & Vogel, P. 1993 Quasielastic neutrino scattering from oxygen and the atmospheric neutrino problem. *Phys. Rev.* D. (In the press.)

Frank, E. D. 1992 A study of atmospheric neutrino interactions in the Kamiokande-II detector. (150 pages.) Ph.D. thesis, University of Pennsylvania.

Frati, W., Gaisser, T. K., Mann, A. K. & Stanev, T. 1993 Atmospheric neutrino data and neutrino oscillations. *Phys. Rev.* D **48**, 1140–1149.

Gaisser, T. K. 1993 Atmospheric neutrino event rates: the expectations. These proceedings.

Gaisser, T. K., Stanev, T. & Barr, G. 1988 Cosmic-ray neutrinos in the atmosphere. *Phys. Rev.* D **38**, 85–95.

Hirata, K. S., *et al.* 1992 Observation of a small atmospheric ν_μ/ν_e ratio in Kamiokande. *Phys. Lett.* B **280**, 146–152.

Hirata, K. S., *et al.* 1988 Experimental study of the atmospheric neutrino flux. *Phys. Lett.* B **205**, 416–420.

Honda, M., Kasahara, K., Hidaka, K. & Midorikawa, S. 1990 Atmospheric neutrino fluxes. *Phys. Lett.* B **248**, 193–198.

Kajita, T. 1993 Observation of a small atmospheric ν_μ/ν_e ratio in Kamiokande and its implications. In *Frontiers of neutrino astrophysics* (ed. K. Nakamura & Y. Suzuki). Tokyo: Universal Academy Press.

Lee, H. & Koh, Y. S. 1990 A new calculation of the atmospheric neutrino flux. *Nuovo Cimento* B **105**, 883–887.

Mann, A. K. 1993 Neutrino cross sections and the small atmospheric ν_μ/ν_e ratio. *Phys. Rev.* D. (In the press.)

Mann, W. A., Kafka, T. & Leeson, W. 1992 The atmospheric neutrino flux ν_μ/ν_e anomaly as a manifestation of proton decay $p \rightarrow e^+\nu\nu$. *Phys. Lett.* B **291**, 200–205.

Mori, M., *et al.* 1991 Search for neutralino dark matter in Kamiokande. *Phys. Lett.* B **270**, 89–96.

Nakahata, M., *et al.* 1986 Atmospheric neutrino background and pion nuclear effect for Kamioka nucleon decay experiment. *J. phys. Soc. Jpn* **55**, 3786–3805.

Oyama, Y., *et al.* 1989 Experimental study of upward-going muons in Kamiokande. *Phys. Rev.* D **39**, 1481–1491.

Perkins, D. H. 1993 The atmospheric neutrino problem: a critique. *Nucl. Phys.* B **399**, 3–14.

Svoboda, R. 1993 Transparencies from the Workshop on Atmospheric Neutrinos, 6–8 May 1993 (ed. R. Svoboda). Louisiana State University Internal Report LSU-HEPA-93-6.

Volkova, L. V. 1980 Energy spectra and angular distributions of atmospheric neutrinos. *Yad. Fiz.* **31**, 1510–1521. (Trans. *Sov. J. Nucl. Phys.* **31**, 784–790.)

Zacek, G., *et al.* 1986 Neutrino oscillation experiments at the Gösgen nuclear power reactor. *Phys. Rev.* D **34**, 2621–2636.

PHILOSOPHICAL TRANSACTIONS OF THE ROYAL SOCIETY A MATHEMATICAL, PHYSICAL & ENGINEERING SCIENCES